*Sensors and Materials*, Vol. 33, No. 6 (2021) 2195–2201
MYU Tokyo



S & M 2607

# VUV- and X-ray-induced Properties of $Lu_2Si_2O_7$, $Y_2Si_2O_7$, and $Gd_2Si_2O_7$ Single Crystals

Prom Kantuptim,[1*] Hiroyuki Fukushima,[1] Hiromi Kimura,[1] Daisuke Nakauchi,[1] Takumi Kato,[1] Masanori Koshimizu,[2] Noriaki Kawaguchi,[1] and Takayuki Yanagida[1]

[1]Division of Materials Science, Graduate School of Science and Technology,
Nara Institute of Science and Technology, 8916-5 Takayama, Ikoma, Nara 630-0192, Japan
[2]Department of Applied Chemistry, Graduate School of Engineering,
Tohoku University, 6-6-07 Aoba, Aramaki, Sendai, Miyagi 980-8579, Japan

(Received January 29, 2021; accepted March 30, 2021)

***Keywords:*** lutetium pyrosilicate, yttrium pyrosilicate, gadolinium pyrosilicate, vacuum ultraviolet, photoluminescence

Undoped $Lu_2Si_2O_7$ (LPS), $Y_2Si_2O_7$ (YPS), and $Gd_2Si_2O_7$ (GPS) single crystals are prepared by the floating-zone (FZ) method. The X-ray diffraction (XRD) patterns show the single phase of each material without any impurity phases. The luminescence properties of the samples are investigated under both vacuum ultraviolet (VUV) and X-ray excitation. When the samples are excited by VUV photons, intrinsic emission bands at 350–500, 320–480, and 310 nm are observed for LPS, YPS, and GPS, respectively. The X-ray-induced scintillation spectra have a similar spectral shape to those under excitation by VUV photons. The X-ray induced scintillation decay times of LPS and YPS are 48 and 13 μs, respectively. For GPS, two scintillation decay constants of 169 μs and 1 ms are observed.

## 1. Introduction

A scintillator is a fundamental part of the monitoring device for ionizing radiation in many industrial and scientific fields including security,[1] well logging,[2] medical diagnostics,[3,4] environmental monitoring,[5] and high-energy physics.[6] Simultaneously, the development of new high-performance scintillator materials is crucial for the advancement of radiation monitoring devices. Plastic,[7] transparent ceramic,[8] glass,[9] crystal,[10,11] and organic–inorganic compounds[12] can be used as scintillators. Typical scintillation materials consist of a host and an emission center (dopant). The former has the function of absorbing the energy from the ionizing radiation, and the latter can convert the absorbed energy to low-energy photons with energy of 1–6 eV.[13] Recently, the combination of rare-earth ions as emission centers and a heavy rare-earth-based host has been considered preferable for scintillators, and a bulk single-crystal form including rare-earth ions in both the emission centers and the host sometimes shows ideal scintillation properties such as high scintillation light yield, fast decay time, good energy resolution, excellent radiation hardness, and high density.[14]

*Corresponding author: e-mail: prom.kantuptim.pf2@ms.naist.jp
https://doi.org/10.18494/SAM.2021.3316

ISSN 0914-4935 

In 2003, Pidol *et al*. introduced Ce-doped $Lu_2Si_2O_7$ (LPS) with a fast decay time of 38 ns and high light yield of 26300 ph/MeV.[15] Since then, the pyrosilicate materials have become among the most attractive host materials for studying novel scintillators, with Nd-, Tm-, and Ce-doped LPS being typical materials.[16–18] In addition to these lanthanide emission centers, $Pr^{3+}$ ions have also been doped to pyrosilicate hosts with the expectation of a faster scintillation decay time than that of Ce-doped hosts due to the $Pr^{3+}$ 5d–4f transition.[19] However, the scintillation spectrum of Pr-doped LPS is not yet fully understood owing to the many crystal structures depending on the chemical composition of the pyrosilicate crystals.[20] Moreover, this complication has also appeared in other pyrosilicate materials such as $Y_2Si_2O_7$ (YPS) and $Gd_2Si_2O_7$ (GPS) when doped with Pr.[21,22] To clarify the emission origins of pyrosilicate scintillators, the study of undoped pyrosilicate crystals is necessary. On the basis of the above background, we investigate in this study the photoluminescence (PL) and scintillation properties of undoped LPS, YPS, and GPS for a deeper understanding of these pyrosilicate materials.

## 2. Materials and Methods

LPS, YPS, and GPS single crystals are prepared as follows. First, appropriate amounts of high-purity powders of $SiO_2$ (99.99%), $Lu_2O_3$ (99.99%) for LPS, $Y_2O_3$ (99.99%) for YPS, and $Gd_2O_3$ (99.99%) for GPS are measured, mixed, and put in a flexible mold. Hydrostatic pressure is applied to each compound for rod shaping, and these rods are sintered at 1200 °C for 8 h. After obtaining the ceramic rods, a crystal is grown by using a quad xenon arc lamp floating zone (FZ) furnace (Crystal Systems Corporation, FZ-T-12000-X-VPO-PC-YH) with a pull-down rate of 10 mm/h.[23] When the crystal growth is finished, single crystals of LPS, YPS, and GPS are cut and polished to 1 mm thickness. The fractions of each sample obtained from the remaining crystalline rods are ground to fine powders for powder X-ray diffraction (XRD) analysis using an X-ray diffractometer (Rigaku, MiniFlex600) in the $2\theta$ range of 10–40°. The X-ray source is a conventional X-ray tube operated at 15 mA and 40 kV with a Cu Kα target.

The PL excitation and emission spectra are measured at room temperature under synchrotron radiation at the UVSOR synchrotron facility (BL-7B), Institute for Molecular Science, National Institutes of Natural Sciences in Aichi, Japan.[24,25] The excitation wavelength is in the vacuum ultraviolet (VUV) region from 50 to 200 nm. The 200–300 nm excitation spectra are measured using a spectrofluorometer (JASCO, FP-8600) with a 440 nm bandpass filter for the LPS and YPS samples and a 325 nm shortpass filter for the GPS sample. The X-ray-induced scintillation properties are observed from the scintillation spectra and decay curves obtained with our original setups.[26,27] In the scintillation decay time measurement, the X-ray tube is operated at a voltage of 40 kV and the detection wavelength is 160–650 nm.

## 3. Results and Discussion

### 3.1 Sample conditions

The sizes of the as-grown single-crystal rods are 4 mm ϕ × 19 mm, 4 mm ϕ × 12 mm, and 5 mm ϕ × 21 mm for the LPS, YPS, and GPS, respectively. Figure 1 shows photographs of the

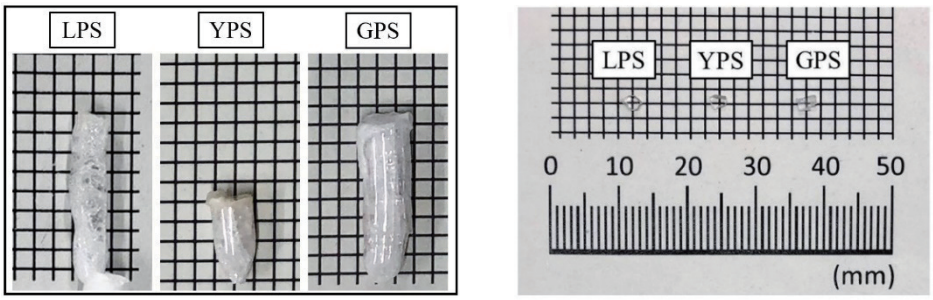


(a) (b)

Fig. 1. (a) As-grown LPS, YPS, and GPS single crystals and (b) cut and polished samples.

as-grown (a) and cut and polished samples (b) used for characterization. Cracks can be found throughout the entire rods. All of the cut and polished samples are colorless, transparent, and crack-free.

Figure 2 presents the XRD patterns of the powdered LPS, YPS, and GPS samples. The XRD peak positions of the LPS, YPS, and GPS samples are matched with the COD 8100597 (monoclinic LPS), JCPDS 82-0732 (orthorhombic YPS), and COD 9011106 (monoclinic GPS) references, respectively. Furthermore, no impurity phases in the $Lu_2O_3$–$SiO_2$, $Y_2O_3$–$SiO_2$, and $Gd_2O_3$–$SiO_2$ phase diagrams are detected within the detection limit of our instrument.[28–30]

### 3.2 PL properties

Figure 3 presents the VUV-excited PL excitation and emission spectra of LPS, YPS, and GPS. The excitation spectra of LPS have two peaks at 174 and 200 nm. In the YPS sample, two excitation bands appear at 150–176 and 194 nm. The emission spectra of LPS and YPS exhibit broad emission at around 350–500 and 320–480 nm corresponding to the two excitation bands, respectively. A similar result occurred in another study on the PL emission of undoped LPS at 10 K, and the emission origin was assigned to be a self-trapped exciton (STE) but without a detailed explanation.[19] Although no detailed information was given, this emission would not have been detected at room temperature in past work since only data at very low temperatures have been presented.[19] From the previous data and our data, the Stokes shift is very large, although differences of a few nm due to differences of the sample and detector can be seen. The spectral shapes of LPS, YPS, and GPS are similar, which means that the main origin of the emission will be the same. Judging from the large temperature dependence (possibly huge thermal quenching at room temperature) and large Stokes shift, this broad emission originates from STE luminescence. The excitation spectra of the GPS sample monitored at 350 nm have two excitation peaks at around 174 and 194 nm with low intensity. The GPS sample has a narrow emission peak at 310 nm, in addition to the same broad emission band as LPS and YPS at 320–420 nm. This narrow emission at 310 nm originates from the $Gd^{3+}$ 4f–4f transition. The GPS sample also has other emissions at 590 and 610 nm. From the spectral shape, these emissions are

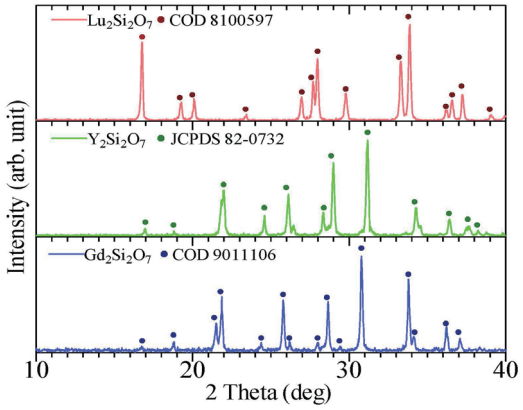


Fig. 2. (Color online) XRD patterns of LPS, YPS, and GPS samples with references.

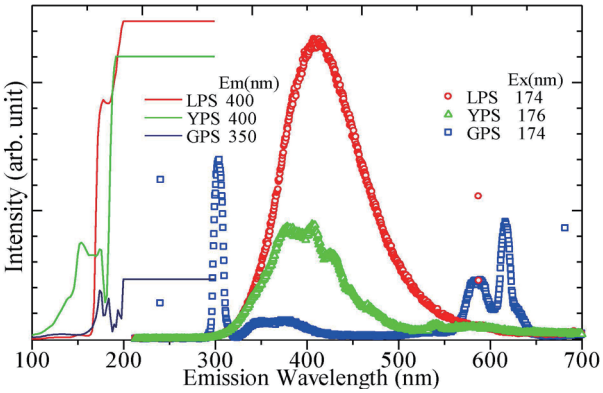


Fig. 3. (Color online) VUV-excited PL excitation and emission spectra of LPS, YPS, and GPS samples.

possibly caused by the $Eu^{3+}$ 4f–4f transition due to the unexpected contamination of $Eu^{3+}$ ions.[11,31] None of the samples show any excitation bands in the 200–300 nm range, as revealed using a common commercial spectrofluorometer, and normalized data are presented as straight horizontal lines in Fig. 3. Unfortunately, the VUV-excited PL decay time cannot be analyzed by the UVSOR (BL-7B) due to the limitation of the 80 ns time range. The VUV-excited PL decay time is very long upon 174–176 nm excitation, as revealed by monitoring at 350 nm, which is consistent with the scintillation decay described later.

### 3.3 Scintillation properties

The X-ray-induced scintillation spectrum of the LPS sample is presented in Fig. 4, which is superposed with that of 1% Pr-doped LPS from our previous study for comparison.[32] The undoped LPS sample exhibits a broad emission band at 350–450 nm, which comes from the STE, similar to the VUV-excited PL emission spectrum (Fig. 3). When comparing this spectrum with the Pr-doped LPS, the emission at 350–450 nm appears for both undoped and Pr-doped LPS. Various origins have been proposed for the 350–450 nm emission, such as the impurity emission from contaminated $Ce^{3+}$[33] and emission from $Pr^{3+}$ in different host crystal structures.[20] From the current investigation, we conclude that the emission around 400 nm in the Pr-doped LPS is likely to be the LPS host emission, possibly the STE. Quenching of the host emission such as the STE by the introduction of some dopant ions also supports our interpretation. The same interpretation also applies for Pr-doped YPS, as shown in Fig. 5.

A similar scintillation characteristic at this wavelength also appears in the Pr-doped GPS. Figure 6 compares the scintillation spectra of the undoped GPS and Pr-doped GPS from one of our previous studies.[22] The same emission peak appears at 310 nm for both samples, which means that the introduction of $Pr^{3+}$ cannot suppress the emission from the $Gd^{3+}$ 4f–4f transition. Very weak emissions accompanied with the emission line due to $Gd^{3+}$ at 310 nm are induced from the $Pr^{3+}$ 5d–4f transition, and the broad emission at around 350 nm is from the STE in both undoped and Pr-doped GPS.

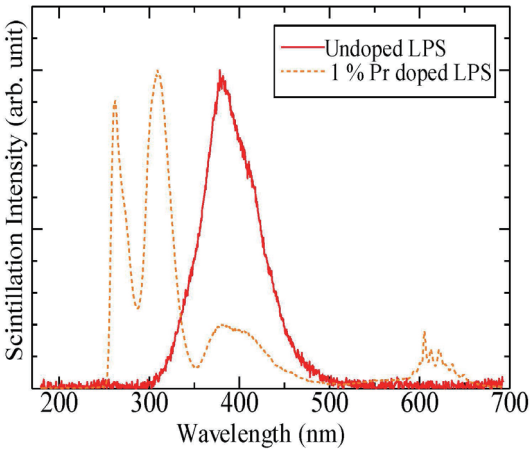


Fig. 4. (Color online) X-ray-induced scintillation spectra of LPS sample and Pr-doped LPS.

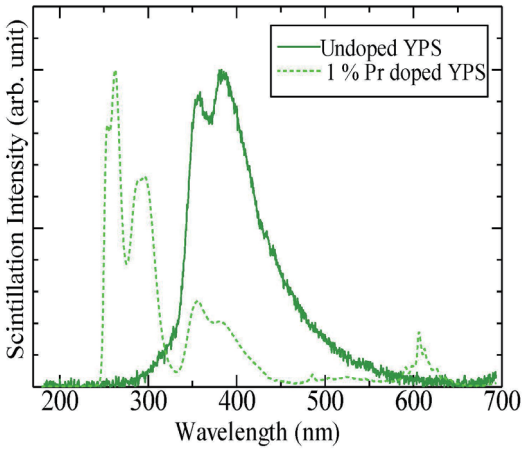


Fig. 5. (Color online) X-ray-induced scintillation spectra of YPS sample and Pr-doped YPS.

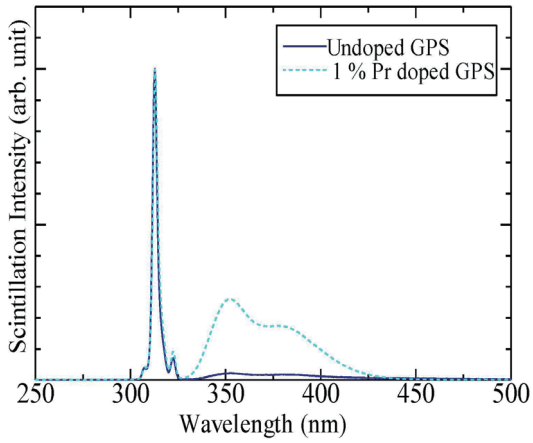


Fig. 6. (Color online) X-ray-induced scintillation spectra of GPS sample and Pr-doped GPS.

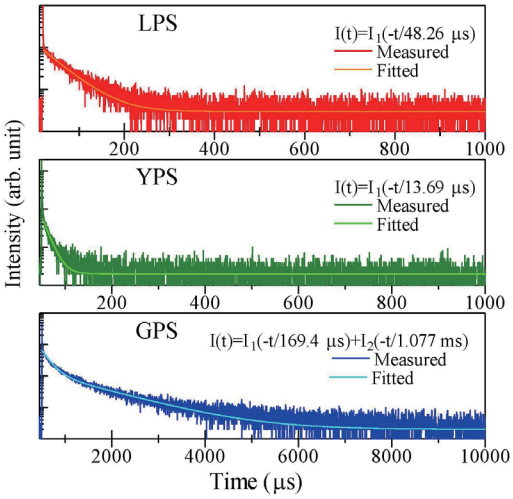


Fig. 7. (Color online) X-ray-induced scintillation decay time profiles of undoped LPS, YPS, and GPS samples.

Figure 7 presents the X-ray-induced scintillation decay time profiles of the LPS, YPS, and GPS samples. For the LPS and YPS samples, the decay time profiles are approximated with a single exponential function, and the decay constants are 48 and 13 μs for LPS and YPS, respectively. For GPS, the decay time profile consists of the sum of two exponential functions with first and second decay constants of 169 μs and 1 ms, respectively. The faster decay is caused by the STE and the slower one is due to the 4f–4f transition of $Gd^{3+}$. The slow scintillation decays of these undoped pyrosilicates are consistent with the VUV-excited PL decay, which cannot be measured within an 80 ns time range.

## 4. Conclusions

Undoped LPS, YPS, and GPS single crystals are successfully synthesized by a quad xenon arc lamp FZ furnace. The XRD pattern of each sample reveals a single phase of LPS, YPS, and GPS without any impurity phases. The VUV-excited PL emission spectra exhibit emission at 350–500, 320–480, and 310 nm for LPS, YPS, and GPS, respectively. Under X-ray irradiation, LPS and YPS exhibit emission at 350–450 and 360–500 nm, respectively, while GPS exhibits a strong and narrow emission line at 310 nm. The X-ray-induced scintillation decay times of LPS and YPS are 48 and 13 μs, respectively. For GPS, two scintillation decay constants of 169 μs and 1 ms are observed. Taking into account all the past works including those by our group, we conclude that the broad emission at 300–500 nm in undoped and doped LPS, YPS, and GPS is caused by the host emission, possibly STE.

## Acknowledgments

This work was supported by the Cooperative Research Project of the Research Center for Biomedical Engineering, Nippon Sheet Glass Foundation, and Japan Society for the Promotion of Science (JSPS) through Grants-in-Aid for Scientific Research A (17H01375) and Scientific Research B (18H03468 and 19H03533).

## References

1 M. Cieślak, K. Gamage, and R. Glover: Crystals **9** (2019) 480.
2 T. Yanagida, Y. Fujimoto, S. Kurosawa, K. Kamada, H. Takahashi, Y. Fukazawa, M. Nikl, and V. Chani: Jpn. J. Appl. Phys. **52** (2013) 3.
3 T. Yanagida, A. Yoshikawa, Y. Yokota, K. Kamada, Y. Usuki, S. Yamamoto, M. Miyake, M. Baba, K. Kumagai, K. Sasaki, M. Ito, N. Abe, Y. Fujimoto, S. Maeo, Y. Furuya, H. Tanaka, A. Fukabori, T. Rodrigues dos Santos, M. Takeda, and N. Ohuchi: IEEE Trans. Nucl. Sci. **57** (2010) 1492.
4 C. Ronda, H. Wieczorek, V. Khanin, and P. Rodnyi: ECS J. Solid State Sci. Technol. **5** (2016) R3121.
5 K. Watanabe, T. Yanagida, and K. Fukuda: Sens. Mater. **27** (2015) 1.
6 M. Kole, M. Chauvin, Y. Fukazawa, K. Fukuda, S. Ishizu, M. Jackson, T. Kamae, N. Kawaguchi, T. Kawano, M. Kiss, E. Moretti, M. Pearce, S. Rydström, H. Takahashi, and T. Yanagida: Nucl. Instrum. Methods Phys. Res., Sect. A **770** (2015) 68.
7 M. Koshimizu, T. Yanagida, R. Kamishima, Y. Fujimoto, and K. Asai: Sens. Mater. **31** (2019) 1233.
8 H. Kimura, T. Kato, D. Nakauchi, M. Koshimizu, N. Kawaguchi, and T. Yanagida: Sens. Mater. **31** (2019) 1265.
9 N. Kawaguchi and T. Yanagida: Sens. Mater. **31** (2019) 1257.
10 N. Kawaguchi, H. Kimura, M. Akatsuka, G. Okada, N. Kawano, K. Fukuda, and T. Yanagida: Sens. Mater. **30** (2018) 1585.
11 D. Nakauchi, N. Kawaguchi, and T. Yanagida: Sens. Mater. **31** (2019) 1249.
12 A. Horimoto, N. Kawano, D. Nakauchi, H. Kimura, M. Akatsuka, and T. Yanagida: Sens. Mater. **32** (2020) 1395.
13 T. Yanagida: Proc. Japan Acad. Ser. B **94** (2018) 75.
14 S. E. Derenzo, M. J. Weber, E. Bourret-Courchesne, and M. K. Klintenberg: Nucl. Instrum. Methods Phys. Res., Sect. A **505** (2003) 111.
15 L. Pidol, A. Khan-Harari, B. Viana, B. Ferrand, P. Dorenbos, J. T. M. De Haas, C. W. E. Van Eijk, and E. Virey: J. Phys. Condens. Matter **15** (2003) 2091.
16 P. Kantuptim, M. Akatsuka, D. Nakauchi, T. Kato, N. Kawaguchi, and T. Yanagida: J. Alloys Compd. **847** (2020) 156542.

17 P. Kantuptim, M. Akatsuka, D. Nakauchi, T. Kato, N. Kawaguchi, and T. Yanagida: J. Alloys Compd. **860** (2020) 158538.
18 M. Koshimizu, T. Yanagida, Y. Fujimoto, and K. Asai: J. Rare Earths **34** (2016) 782.
19 L. Pidol, B. Viana, A. Kahn-Harari, A. Bessire, and P. Dorenbos: Nucl. Instrum. Methods Phys. Res., Sect. A **537** (2005) 125.
20 T. Yanagida, K. Watanabe, G. Okada, and N. Kawaguchi: Jpn. J. Appl. Phys. **57** (2018) 106401.
21 P. Kantuptim, M. Akatsuka, N. Kawaguchi, and T. Yanagida: Jpn. J. Appl. Phys. **59** (2020) SCCB17.
22 P. Kantuptim, M. Akatsuka, D. Nakauchi, T. Kato, N. Kawaguchi, and T. Yanagida: Sens. Mater. **32** (2020) 1357.
23 D. Nakauchi, G. Okada, N. Kawaguchi, and T. Yanagida: Jpn. J. Appl. Phys. **57** (2018) 100307.
24 K. Fukui, H. Nakagawa, I. Shimoyama, K. Nakagawa, H. Okamura, T. Nanba, M. Hasumoto, and T. Kinoshita: J. Synchrotron Radiat. **5** (1998) 836.
25 K. Fukui, H. Miura, H. Nakagawa, I. Shimoyama, K. Nakagawa, H. Okamura, T. Nanba, M. Hasumoto, and T. Kinoshita: Nucl. Instrum. Methods Phys. Res., Sect. A **467–468** (2001) 601.
26 T. Yanagida, K. Kamada, Y. Fujimoto, H. Yagi, and T. Yanagitani: Opt. Mater. **35** (2013) 2480.
27 T. Yanagida, Y. Fujimoto, T. Ito, K. Uchiyama, and K. Mori: Appl. Phys. Express **7** (2014) 62401.
28 X. Ye, Y. Luo, S. Liu, D. Wu, D. Hou, and F. Yang: J. Rare Earths **35** (2017) 927.
29 H. Mao, M. Selleby, and O. Fabrichnaya: Calphad **32** (2008) 399.
30 V. Baumer, I. Gerasymov, O. Sidletskiy, O. Voloshina, and S. Neicheva: J. Alloys Compd. **509** (2011) 8478.
31 Y. Shi, Q. W. Chen, and J. L. Shi: Opt. Mater. **31** (2009) 729.
32 P. Kantuptim, M. Akatsuka, D. Nakauchi, T. Kato, N. Kawaguchi, and T. Yanagida: Radiat. Meas. **134** (2020) 106320.
33 M. Nikl, A. M. Begnamini, V. Jary, D. Niznansky, and E. Mihokova: Phys. Status Solidi: Rapid Res. Lett. **3** (2009) 293.